Title

Identification of long non-coding RNAs in Verticillium dahliae following inoculation of cotton.

Authors

Li, Ran
Xue, Hui-Shan
Zhang, Dan-Dan
et al.

Publication Date

2022-04-01

DOI

10.1016/j.micres.2022.126962

Peer reviewed

Microbiological Research 257 (2022) 126962

Contents lists available at ScienceDirect

Microbiological Research

journal homepage: www.elsevier.com/locate/micres

Identification of long non-coding RNAs in *Verticillium dahliae* following inoculation of cotton

Ran Li [a], Hui-Shan Xue [a], Dan-Dan Zhang [a], Dan Wang [a], Jian Song [a], Krishna V. Subbarao [b], Steven J. Klosterman [c,*], Jie-Yin Chen [a,*], Xiao-Feng Dai [a,*]

[a] State Key Laboratory for Biology of Plant Diseases and Insect Pests, Institute of Plant Protection, Chinese Academy of Agricultural Sciences, Beijing, 100193, China
[b] Department of Plant Pathology, University of California, Davis, c/o U.S. Agricultural Research Station, Salinas, CA, United States
[c] United States Department of Agriculture, Agricultural Research Service, Crop Improvement and Protection Research Unit, Salinas, CA, United States

ARTICLE INFO

Keywords:
lncRNA
Verticillium wilt
Verticillium dahliae
Neighbor genes
Virulence

ABSTRACT

Long non-coding RNAs (lncRNAs) play important roles in diverse biological processes. However, these functions have not been assessed in *Verticillium dahliae*, a soil-borne fungal pathogen that causes devastating wilt diseases in many crops. The discovery and identity of novel lncRNAs and their association with virulence may contribute to an increased understanding of the regulation of virulence in *V. dahliae*. Here, we identified a total of 352 lncRNAs in *V. dahliae*. The lncRNAs were transcribed from all *V. dahliae* chromosomes, typically with shorter open reading frames, lower GC content, and fewer exons than protein-coding genes. In addition, 308 protein-coding genes located within 10 kb upstream and 10 kb downstream of lncRNAs were identified as neighboring genes, and which were considered as potential targets of lncRNA. These neighboring genes encode products involved in development, stress responses, and pathogenicity of *V. dahliae*, such as transcription factors (TF), kinase, and members of the secretome. Furthermore, 47 lncRNAs were significantly differentially expressed in *V. dahliae* following inoculation of susceptible cotton (*Gossyoiumhisutum*) cultivar Junmian No.1, suggesting that lncRNAs may be involved in the regulation of virulence in *V. dahliae*. Moreover, correlations in expression patterns between lncRNA and their neighboring genes were detected. Expression of *lncRNA012077* and its neighboring gene was up-regulated 6 h following inoculation of cotton, while the expression of *lncRNA007722* was down-regulated at 6 h but up-regulated at 24 h, in a pattern opposite to that of its neighboring gene. Overexpression of *lncRNA012077* in wild-type strain (Vd991) enhanced its virulence on cotton while overexpression of *lncRNA009491* reduced virulence. Identification of novel lncRNAs and their association with virulence may provide new targets for disease control.

1. Introduction

Long noncoding RNAs (lncRNAs) have emerged as crucial factors regulating key biological processes in various eukaryotes. LncRNAs are transcribed primarily by RNA polymerase II and are longer than 200 nucleotides (Guttman et al., 2013). Antisense lncRNAs exert their regulatory effects on corresponding sense mRNAs via epigenetic regulation, chromatin remodeling, RNA-RNA interactions, and post-transcriptional mechanisms, including regulation of mRNA processing and transport (Beaulieu et al., 2012). Additional common characteristics of lncRNAs include their reduced conservation and expression levels relative to coding genes. Although typically lncRNAs have no protein coding potential, lncRNAs may occasionally function as protein-coding genes (Anderson et al., 2015; Nelson et al., 2016).

The prevalence of lncRNAs has been reported in many eukaryotes including mammals, plants, and fungi. The most prominent examples of lncRNAs are those from mammals that affect epigenetic regulation of X-chromosome inactivation, genomic imprinting, stem cell pluripotency, development, cancer metastasis, and other biological processes (Ulitsky and Bartel, 2013). The functional characterizations of the mechanisms of action by lncRNA in plants, however, are lagging. Plant lncRNAs have been implicated in flowering time control (Csorba et al., 2014), gene

Abbreviations: lncRNA, Long noncoding RNAs; DELs, Differentially expressed lncRNAs; GO, Gene ontology; KEGG, Kyoto encyclopedia of genes and genomes; CAZy, Carbohydrate-active enZymes; SCRP, Secreted cysteine-rich protein; TF, Transcription factor; PHI, Pathogen-host interaction; ORF, Open reading frame.

* Corresponding authors.
E-mail addresses: steve.klosterman@usda.gov (S.J. Klosterman), chenjieyin@caas.cn (J.-Y. Chen), daixiaofeng_caas@126.com (X.-F. Dai).

https://doi.org/10.1016/j.micres.2022.126962
Received 23 May 2021; Received in revised form 20 December 2021; Accepted 4 January 2022
Available online 6 January 2022

silencing (Wu et al., 2018), fruit ripening (Li et al., 2018a, 2018b), abiotic stress responses (Qin et al., 2017), innate immune responses (Seo et al., 2019), and reproduction (Wang et al., 2018). Several lncRNAs have been identified in *Arabidopsis* that were expressed in response to *Fusarium oxysporum* infection (Zhu et al., 2014) and in cotton associated with resistance to *Verticilliumdahliae* (Zhang et al., 2018a, 2018b).

Although many lncRNAs have been identified from sequence data, only a few lncRNAs are functionally well characterized in fungi. Fungal lncRNAs are involved in various cellular processes such as meiosis, telomere synthesis and maintenance, metabolism, sexual reproduction, conidiation, and stress responses (Tang et al., 2021; Till et al., 2018; Wang et al., 2021). In *Saccharomycescerevisiae*, the lncRNA *IRT1* inhibits expression of *inducer of meiosis 1* (*IME1*) to prevent germ cell differentiation and sporulation in haploids (van Werven et al., 2012) and two telomere-associated lncRNAs have been identified, namely *TERRA* and *TLC1* (Luke et al., 2008; Zappulla and Cech, 2004). *TERRA* acts as a scaffold for telomeric DNA and chromatin-modifying enzymes during telomere synthesis and regulates telomerase activity (Luke et al., 2008). Furthermore, *TLC1* provides a platform for the formation of the telomerase complex itself and serves as a template for reverse transcription (Zappulla and Cech, 2004). The lncRNA *HAX1* in *Trichoderma reesei* was tightly associated with cellulase expression which can interact with transcriptional activator *Xyr1* to negatively regulate the expression of *Xyr1* (Till et al., 2020). In addition, some lncRNAs play important roles in pathogenicity and growth of fungal plant pathogens. For example, *UvlncNAT-MFS* participates in the regulation of *Ustilaginoidea virens* growth, conidiation, and various stress responses by forming RNA duplexes with *UvMFS* (Tang et al., 2021). *GzmetE* encodes a homoserine *O*-acetyltransferase which is important for sexual development and plant infection by *Fusarium graminearum*. *GzmetE-AS* is a natural antisense lncRNA, transcribed from the opposite strand of *GzmetE* and was identified as participating in asexual and sexual reproduction by regulating the expression of *GzmetE* (Wang et al., 2021).

V. dahliae is a widely distributed soilborne pathogenic fungus that infects the roots and invades xylem vessels of susceptible plants, causing an intractable vascular wilt disease (Fradin and Thomma, 2006; Klimes et al., 2015). The profiles and the function of resistance-associated lncRNAs in two different cotton species, *Gossypiumbarbadense* and *G. hirsutum*, following inoculations with *V. dahliae* have been reported (Zhang et al., 2018a, 2018b). Comparative genomics of *V. dahliae* isolates from cotton, lettuce, and tomato has yielded insights into the genetic basis of pathogen colonization, host adaptability, and evolution of asexuality (Chen et al., 2018; Klosterman et al., 2011; de Jonge et al., 2013). The availability of increasing numbers of genome sequences and their analyses has also effectively promoted the screening and identification of numerous developmental and pathogenicity-related genes (Klimes et al., 2015). However, in spite of the widespread availability of these sequences, no lncRNAs have been identified or characterized in any functional capacity in *V. dahliae*. Over 50 % of the *V. dahliae* genome is non-coding, indicating ample space for the transcription of lncRNAs in *V. dahliae* (Chen et al., 2018). In this study, we aimed primarily to identify lncRNAs from *V. dahliae* following inoculation of cotton roots that may be involved in the infection process. Potential functions of *V. dahliae* lncRNAs were identified based on expression analyses and examinations of neighboring genes, including the finding that some of the lncRNA-neighboring genes are associated with roles in development, stress responses, and pathogenicity, and thus may shed light on lncRNA regulatory roles in *V. dahliae*.

2. Materials and methods

2.1. Plant and fungal pathogen and inoculations

The susceptible cotton *G.hirsutum* cultivar Junmian No.1 (cv. Junmian No.1) was planted in autoclaved potting mix at 28 ℃ with 16 h light/8 h dark for 2 weeks and used for inoculations. *V. dahliae* isolate Vd991 (Chen et al., 2018), a highly aggressive defoliating strain, was cultured in complete medium (CM) at 25 ℃ for 5 days. Conidia were harvested from the cultures and concentrated by centrifugation, washed with sterile water, and the inoculum suspension with the final concentration adjusted to 5×10^6 conidia/ml was used for inoculating cotton seedlings (Li et al., 2018a, 2018b). Roots of the seedlings were immersed in the conidial suspension, and conidia were sampled at 0 h, 6 h, and 24 h post-inoculation. Conidia of Vd991 in the suspension not used for inoculation were used as the control treatment. Three replicate experiments were performed, and each replicate included 6 seedlings. Conidia of Vd991 were collected by gentle centrifugation at 4000 revolutions per min for 5 min. All samples were immediately frozen in liquid nitrogen and stored at -80 ℃ until use.

2.2. RNA library construction and sequencing

Total RNA samples of *V. dahliae* were extracted using an RNA Purification Kit (Tiangen, Beijing, China) and prepared for sequencing with three biological replicates for each sample. Genomic DNA was removed by DNase treatment, and rRNA was removed by Ribo-zero™ rRNA Removal Kit (Epicenter, USA). Strand-specific sequencing was performed on an Illumina HiSeq X-Ten by BGI (BGI-genomics, Shenzhen), which generated 125 bp paired-end reads. Raw data were processed through in-house perl scripts to obtain clean reads. The clean reads were obtained by removing the adapter and low-quality reads (quality score > Q20). Over 15 gigabases of clean data were generated from each sample. The data presented in this article have been deposited in the National Center for Biotechnology Information (NCBI) Sequence Read Archive (http://www.ncbi.nlm.nih.gov/sra/, accession number is PRJNA735544). The clean reads were mapped onto the reference genome of *V. dahliae* strain Vd991 (GenBank: NVYA01000001.1) by Tophat2 (v2.0.9) (Kim et al., 2013) and Bowtie 2 (v2.2.9) (Langmead and Salzberg, 2012).

2.3. Differential expression analysis of lncRNAs during Vd991 infection

A total of six samples were selected for sequencing, including Vd991 inoculated on cotton at 0 h, 6 h, and 24 h as the treatment (T) group and conidia of Vd991 in the same suspension at 0 h, 6 h, and 24 h but non-inoculated as the control (C) group. Significantly differentially expressed lncRNAs (DELs) were identified from five comparisons, including T6/C0, T24/C0, T6/C6, T24/C6, T24/C24. Fragments Per Kilobase of the transcript, per Million mapped reads (FPKM) was used to determine expression values. Cuffdiff (v2.1.1) was used to calculate the FPKM of lncRNAs in each sample (Trapnell et al., 2010). The fold-change in gene expression value was calculated by FPKM treat/FPKM control. Transcripts were identified as differentially expressed between treatment and control with parameters of fold change >2.0 and *P*-value <0.05.

2.4. RNA extraction and reverse transcription-quantitative PCR (RT-qPCR)

Total RNA was extracted from *V. dahliae* by Plant RNA Purification Kit (Tiangen, Beijing, China). The RNA elutions were stored at -80 ℃ until use. RNA aliquots of 2 μg were used for cDNA synthesis by the TranScript One-Step gDNA Removal and cDNA Synthesis SuperMix kit (Trans, Beijing, China). RT-qPCR was performed using a qPCR SYBR premix Ex TaqII kit (TaKaRa, Tokyo, Japan). The relative quantification of RT-qPCR was measured by the $2^{-\Delta\Delta Ct}$ analysis method. The mRNA expression levels were normalized using *V. dahliae* elongation factor *VdEF-1α* (Gui et al., 2017). Three biological replicates were performed for each experiment, with three technical replicates. The specific primers used are listed in Table S1.

2.5. Gene Ontology (GO) enrichment and KEGG pathways analysis

A total of 308 neighboring protein-coding genes located within 10 kb up- and downstream of lncRNAs were used for functional analysis. Gene Ontology (GO) enrichment analyses were performed by WEGO (http://wego.genomics.org.cn/), filtering the predicted proteins based on their grouping to cellular component, molecular function, and biological function. KEGG enrichment analysis was then performed in KEGG Mapper (https://www.kegg.jp/kegg/mapper.html; Kanehisa et al., 2019).

2.6. Statistical analysis

Data were analyzed using SPSS (version 20.0) software. Analyses of variance followed by mean separation by Duncan's multiple range test was calculated for three or more data sets. Statistically significant differences ($P < 0.05$) are indicated by different lowercase letters in the figures. Pairwise *t*-test was used to test differences between two data sets and levels of significances are shown by the probabilities associated with the test (* indicates $P < 0.05$, ** indicates $P < 0.01$, *** indicates $P < 0.001$).

2.7. Fungal transformations

Sequence of lncRNAs were obtained from RNA-seq data. The full-length sequences of lncRNAs were synthesized and inserted into pUC57 with Kanamycin resistance (Sangon, Beijing, China). Specific primers were designed to clone the lncRNA and the fragment of lncRNA was cloned into the pCOM-TrpC vector for generation of overexpression transformants by the *Agrobacterium*-mediated transformation described previously (Gui et al., 2017).

2.8. Pathogenicity assays

Overexpression transformants and wild type strains were cultured in CM medium at 25 ℃ for 5 days. Conidia were harvested from the cultures and concentrated by centrifugation, washed with sterile water, and the inoculum suspension with the final concentration adjusted to 5×10^6 conidia/ml was used for inoculating 2-wk-old cotton seedlings by root-dip method (Gui et al., 2017). The roots of cotton were harvested at 21 days postinoculation when disease symptoms appeared for genomic DNA extraction. Fungal biomass quantification was detected by amplification of *V. dahliae* elongation factor *VdEF-1α* normalized by the cotton *18S* gene through qPCR.

3. Results

3.1. Genome-wide discovery of lncRNAs in Verticillium dahliae during infection on cotton

To identify lncRNAs in *V. dahliae*, RNA-seq reads of transcripts from *V. dahliae* strain Vd991 were cataloged for both the control and treatment samples that were non-inoculated or inoculated on cotton, respectively. All clean reads were mapped onto the *V. dahliae* genome, and approximately 50 % of clean reads were uniquely mapped to the genome of *V. dahliae* (Table S2). First, 38,254 unique transcripts were assembled from high-throughput RNA-seq data (Fig. 1). To distinguish lncRNAs, four sequential stringent filters of the 38,254 transcripts were employed. Transcripts shorter than 200 nucleotides were discarded, recovering 37,446 transcripts (Fig. 1). Next, the "background" transcripts with an expression threshold of less than two with one exon were excluded, yielding 24,338 transcripts (Fig. 1). The mRNA precursors and transcripts that overlap with known genes on the positive strand were discarded to obtain 7,688 transcripts. Transcripts predicted to encode proteins were further filtered by comparing them with three protein-coding tools (CPC2, CNCI, and Pfam), and finally, 352 lncRNAs were obtained and defined as *V. dahliae* lncRNAs (Fig. 1).

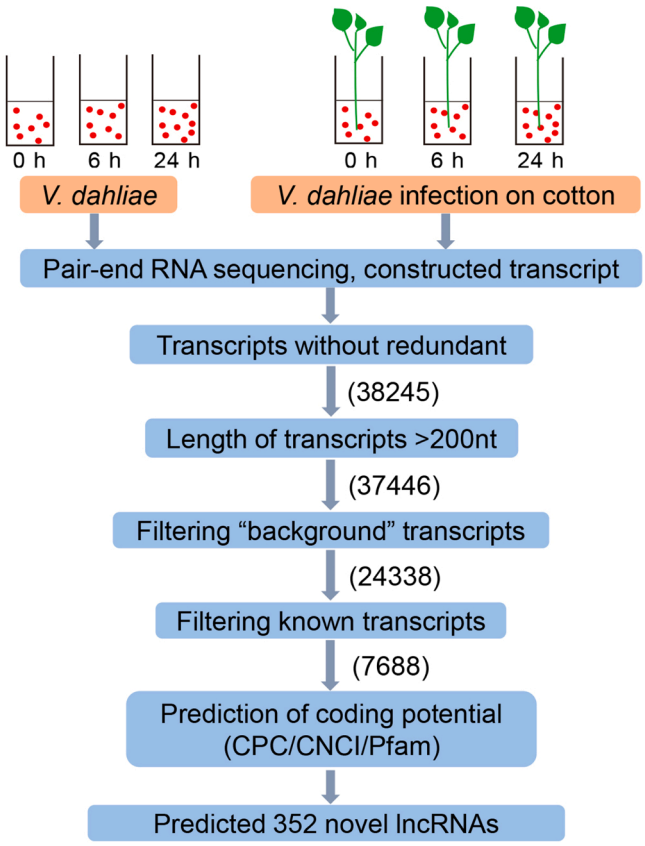

Fig. 1. Schematic diagram of the informatics pipeline for identification of long noncoding RNAs (lncRNAs) in *Verticillium dahliae*.

3.2. Characteristics of Verticilliumdahliae lncRNA

To determine whether *V. dahliae* lncRNAs are shorter and harbor fewer exons than protein-coding genes, we compared the distribution of length and exon numbers of 352 lncRNAs with all *V. dahliae* predicted protein-coding transcripts (10,286 genes from the DK149 genome, assembled at the chromosome level, https://db.cngb.org/VerticilliOmics/). Among the lncRNAs, 80 % ranged from 200 to 1000 nucleotides, with only 20 % longer than 1000 nucleotides. In contrast, about 62 % of the protein-coding genes were longer than 1000 nucleotides (Fig. 2A). The average length of lncRNAs was 303 bp; by contrast, the average length of mRNAs was 3628 bp in the genome of DK149 (Fig. 2A). In addition, the analysis of exon number distribution revealed that lncRNAs mostly contained one or two exons, while protein-coding genes ranged from those containing one to more than ten exons (Fig. 2B). LncRNAs typically have no protein-coding potential, and the results revealed that the length of ORFs within lncRNAs was significantly shorter than those of protein-coding genes (Fig. 2A and C). GC content, which reflects the biased intergenomic nonreciprocal DNA exchanges, was investigated for lncRNAs (Guo et al., 2014). The results revealed that lncRNAs exhibited significantly lower GC content than those of protein-coding genes (Fig. 2D). Above all, *V. dahliae* lncRNAs possessed fewer exons, had lower GC%, and shorter protein-coding genes.

3.3. Distribution between lncRNAs and functional factors in the Verticilliumdahliae genome

Next, the lncRNAs were mapped onto the *V. dahliae* genome of DK149. Their distribution on chromosomes was examined by density in

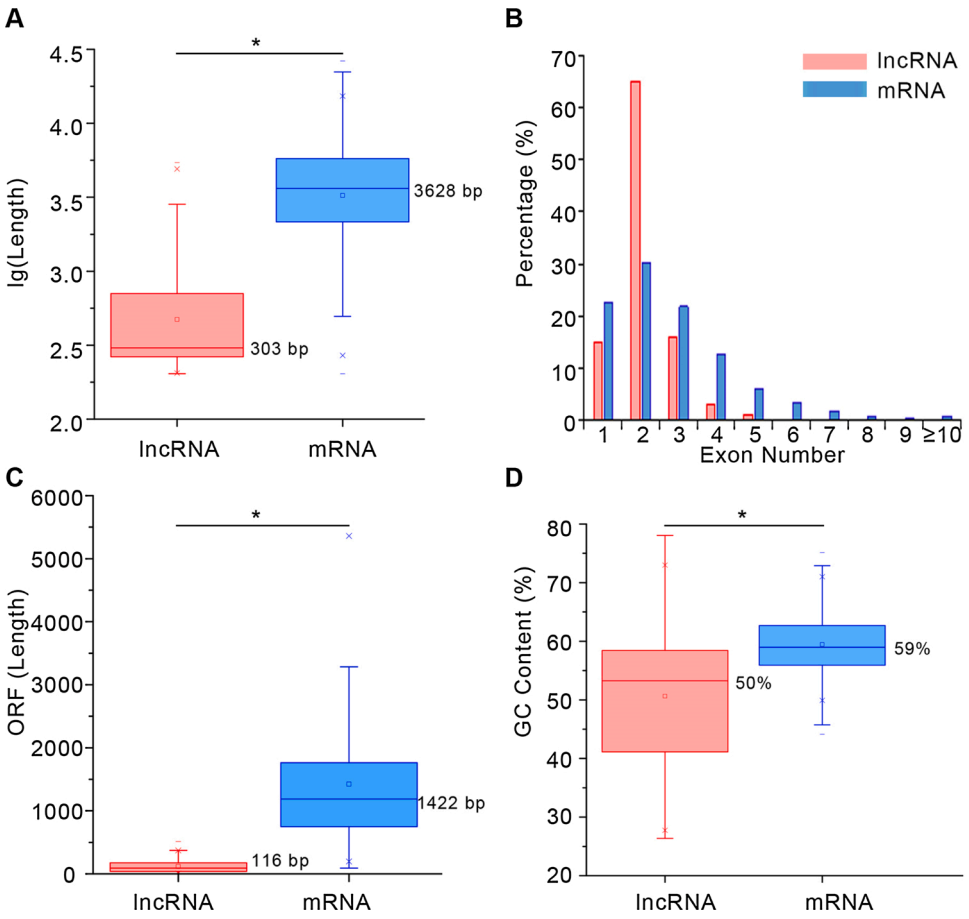

Fig. 2. Characteristics of long noncoding RNAs (lncRNAs) in *Verticillium dahliae*. **(A)** The distribution of the lengths of lncRNAs in comparison with protein-coding genes. **(B)** The number of exons of lncRNAs in comparison with protein-coding genes. **(C)** The length of open reading frames of lncRNAs in comparison with those of protein-coding genes. **(D)** The GC content of lncRNAs and protein-coding genes. $*P < 0.05$

windows of 20 kb. The results revealed an uneven distribution on each chromosome, similar to that observed for protein-coding genes (Fig. 3A). However, the average density of lncRNA (0.997) among chromosomes was significantly lower than genes (29.119). In addition, the density of lncRNAs on chromosome 8 was 37.083, which was higher than on other chromosomes (Fig. 3A). From the sequencing data, we further observed that the proportion of lncRNAs transcribed from chromosome 8 were transcribed from the same locus but in different lengths or in different directions, suggesting that there were several clusters of lncRNAs. Moreover, the density of expressed genes encoding pathogen-host interaction (PHI) proteins, transcription factors (TF), Carbohydrate-Active enZymes (CAZy), small secreted cysteine-rich proteins (SCRP), long terminal repeats (LTR), transposons, and components of the secretome were also analyzed, indicating an uneven distribution (Fig. 3A). Since lncRNAs preferentially regulate expression levels of neighboring genes (Villegas and Zaphiropoulos, 2015), we identified neighboring genes as the protein-coding genes that were located within 10 kb upstream and 10 kb downstream of lncRNAs for further analysis (Cabili et al., 2011), yielding 308 neighboring genes (Table S3). Results showed that the neighboring genes of lncRNAs were associated with the secretome, SCRPs, CAZys, and TFs (Fig. 3B and Table S4). A total of 134 of these genes were identified as PHI, making up 43.51 % of 308 potential lncRNA-associated genes (Fig. S1A). In contrast, the PHI genes account for 26.73 % of the whole DK149 genome (Fig. S1B). In addition, the percentage of cellulose, kinase, and TFs in lncRNA-associated genes was higher than in the whole DK149 genome (Fig. S1). Among the neighboring CAZy-type genes, there were carbohydrate-binding modules (CBM), auxiliary activities (AA), glycoside hydrolases (GH), glycosyl transferases (GT), and carbohydrate esterases (CE) (Fig. 3C). Also detected were different types of TFs (Fig. 3D). Hence, if neighboring genes are under regulatory control of lncRNAs, some of these may be associated with pathogenicity in *V. dahliae*.

3.4. *Identification the putative function of lncRNAs in Verticilliumdahliae*

To investigate the specific functions of lncRNAs, we compared the expression levels of 308 neighboring genes of the lncRNAs in Vd991 following inoculation of cotton relative to the non-inoculated control (Zhang et al., 2019). A total of 106 genes were specifically expressed, including 39 that were up-regulated and 67 that were down-regulated (Table S5). Gene ontology (GO) analyses for lncRNA-associated genes, including biological processes, molecular functions, and cellular components were performed (Table S6). The results showed that genes were primarily classified in binding, catalytic activity, metabolic process, and cellular process. For the term catalytic activity, the majority of genes were involved in hydrolase, oxidoreductase, transferase, kinase, lyase, and ligase activities (Fig. 4A). For the term binding, genes including ATP, oxygen, carbohydrate, and NAD binding (Fig. 4B). Within metabolic processes, genes were classified in regulating methylation, secondary metabolite biosynthetic processes, and regulation of primary metabolic processes (Fig. 4C). Within the category of cellular localization, genes encoded products predicted as associated with organelles and membrane, such as chromosomal mitochondrial membrane and plasma membrane (Fig. 4D). Furthermore, there were a number of genes detected as having products involved in catalytic complexes (Fig. 4D),

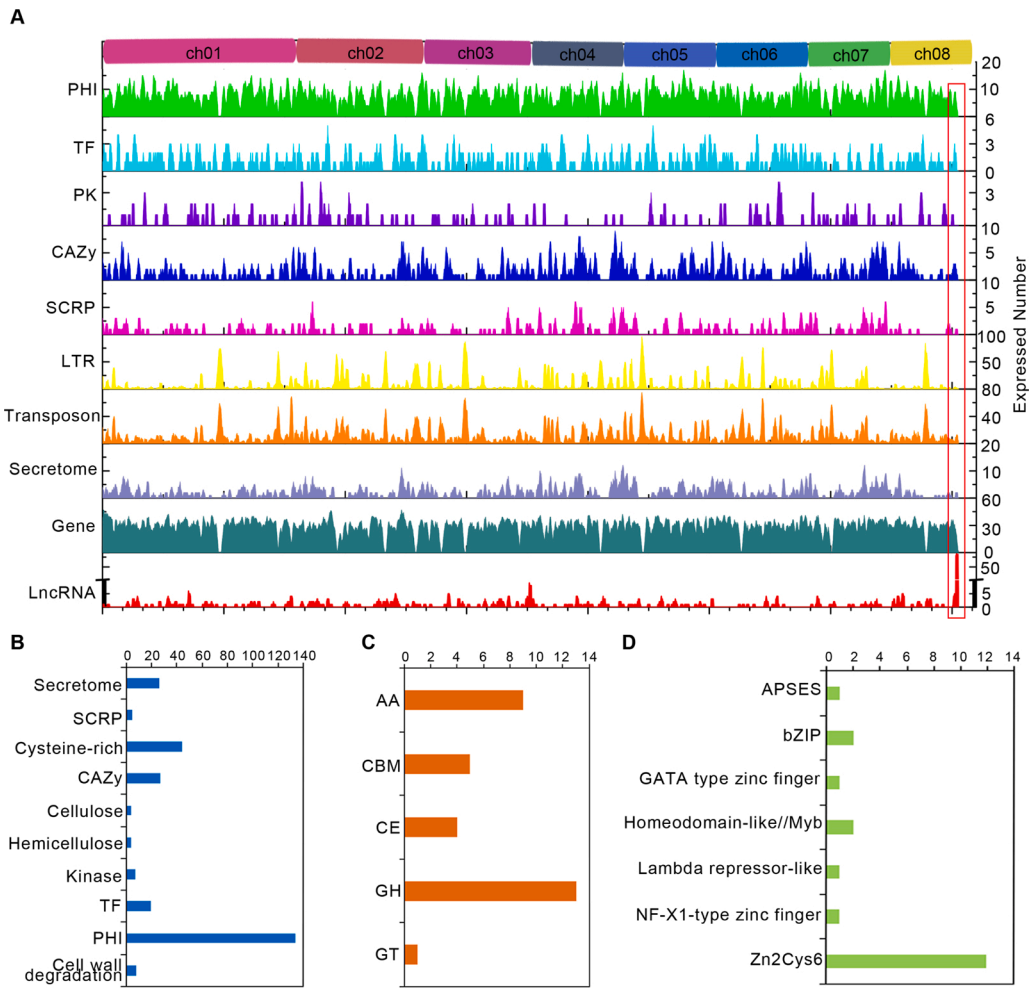

Fig. 3. Genome-wide distribution of long noncoding RNAs (lncRNAs) of *Verticillium dahliae* and analyses of neighboring genes. (A) Genome-wide distribution of *V. dahliae* lncRNAs compared with the distribution of protein-coding genes, secretome, transposons, long terminal repeated (LTR), small secreted cysteine-rich protein (SCRP), Carbohydrate-Active enZymes (CAZy), PK, transcription factor (TF), and pathogen host interaction (PHI). **(B)** Number of neighboring genes associated with potential functional factors in pathogenicity. **(C)** Number of different types of CAZys. **(D)** Number of different types of TFs.

and those related to response to stimuli, including stress and chemicals (Table S6).

KEGG (Kyoto Encyclopedia of Genes and Genomes) (Kanehisa et al., 2019) was used to analyze the potential pathways of the lncRNA-associated genes. A total of 81 pathways were defined, including those of metabolism, cell cycle, amino acid biosynthesis, and others (Table S7). Twenty-two genes were identified as involved in starch and sucrose metabolism and of D-glucose biosynthesis (Fig. 5A). Under cell wall stress, several lncRNA-associated genes included those with functions in the mitogen-activated protein kinase (MAPK) signaling pathway (Fig. 5B). The MAPK signaling pathway is activated by a number of extra and intracellular stimuli, including cytokines, growth factors, and hormones, as well as stressors such as oxidative and endoplasmic reticulum (ER) stress. This pathway plays a key role in the regulation of many cellular processes, including proliferation, differentiation, stress response, motility, growth, survival, and death (Sun et al., 2015). Above all, these results indicated the identified lncRNAs in *V. dahliae* might regulate diverse processes relating to development, signaling, stress responses, and virulence.

3.5. Identification of differentially expressed lncRNAs in the Verticilliumdahliae-cotton interaction

To discover lncRNAs potentially involved in pathogenicity, we compared the levels of lncRNAs between control (C) at 0 h, 6 h, and 24 h and treatment (T) groups at 0 h, 6 h, and 24 h. Significantly differentially expressed lncRNAs (DELs) were identified from five comparisons, including T6/C0, T24/C0, T6/C6, T24/C6, T24/C24. There were 29, 39, 5, 11, and 1 DELs from these comparisons, respectively (Fig. 6A). Four DELs were found among the T6/C0, T24/C0, T6/C6, T24/C6 comparisons (Fig. 6A). A total of 47 DELs were detected after inoculation following a serial analysis method (Fig. 6A). The list of DELs was shown in Table S8. The up- and down-regulated DELs in different combinations are shown in Fig. 6B. In addition, there were 53 neighboring genes of DELs, including those encoding components of the secretome, SCRPs, CAZys, TFs, and PHIs (Table 1). Among the neighboring genes, 21 were significantly expressed in Vd991 when inoculated on cotton than the control (Zhang et al., 2019), yielding 11 up-regulated and 10 down-regulated (Table S9). These results indicated that these lncRNAs might play regulatory roles of pathogenicity-related genes during infection.

3.6. Expression analysis between Verticilliumdahliae lncRNAs and their neighboring genes at early stages of cotton infection

To confirm the expression pattern of lncRNA during infection, we selected four lncRNAs to verify their expression patterns by RT-qPCR at 0, 6, and 24 h after inoculation. Primers for RT-qPCR analysis were designed specifically to distinguish lncRNAs and their overlapping genes because some lncRNAs were located on protein-coding genes. *LncRNA012077* was located on *V010255* and upstream of *V010256* (Fig. 7A). Expression of *lncRNA012077* was up-regulated following inoculation of cotton, as also the expression of *V010255* (Fig. 7B), which encodes a gene involved in oxygen carrier activity. The expression of *V010256* did not significantly change (Fig. 7B). Similarly, *lncRNA011440* overlapped with *V009713* and upstream of *V009714*

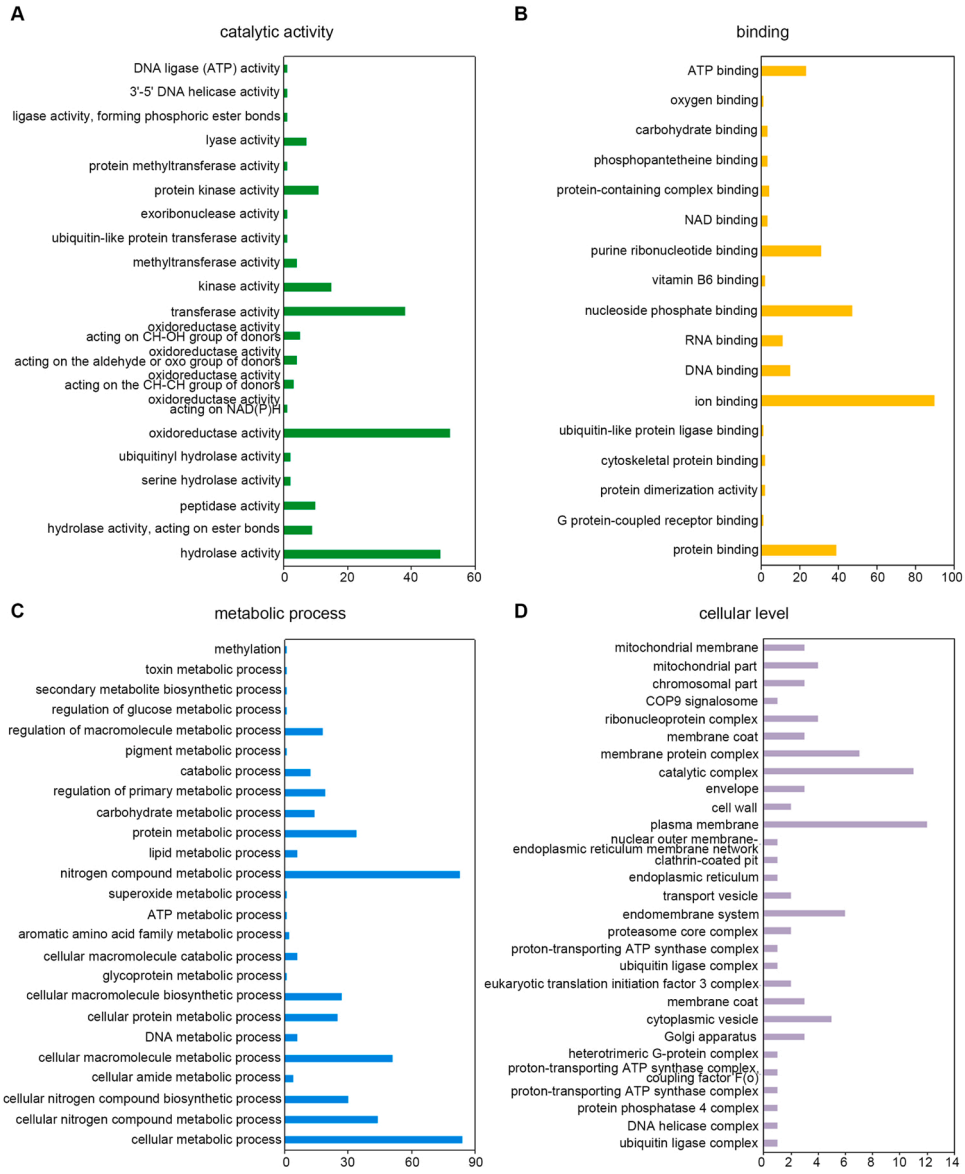

Fig. 4. Gene Ontology (GO) analyses of putative long noncoding RNAs (lncRNAs) *cis*-targeted genes in *Verticillium dahliae*. (**A**) catalytic activity, (**B**) binding, (**C**) metabolic process, and (**D**) cellular level.

(Fig. 7C). The expression level of *lncRNA011440* was significantly upregulated in the treatment group inoculated on cotton, but the expression level of two neighboring genes (*V009713* and *V009714*) was not significantly different (Fig. 7D). The intron of *lncRNA007991* contained *V006984*, and *lncRNA007991* located downstream of *V006985* (Fig. 7E). The expression pattern of *lncRNA007991* was also significantly up-regulated in the treatment group inoculated on cotton (Fig. 7F). Meanwhile, the expression of *V006984* and *V006985* up- and down-regulated, respectively (Fig. 7F). The expression of *lncRNA007722* was down-regulated at 6 h and up-regulated at 24 h (Fig. 7H). Analyses of the expression of *V006398*, encoding a glutathione *S*-transferase gene was opposite to the pattern of *lncRNA007722*, down-regulated at 24 h and up-regulated at 6 h (Fig. 7G and H). The secondary structure of lncRNAs were highly conserved, which may be related to their biological functions (Johnsson et al., 2014; Li et al., 2016; Mercer and Mattick, 2013). The secondary structure of these four lncRNAs was predicted by the RNA fold prediction tool, RNAfold WebServer (Fig. S2). These results indicated that lncRNAs are present in *V. dahliae* and that their expression patterns correlate with early phases of interactions with cotton roots.

3.7. Role of lncRNAs in Verticilliumdahliaepathogenicity

To assess the pathogenic function of *V. dahliae* lncRNAs, we generated lncRNA overexpressing (OE) transformants driven by the *TrpC* promoter. We introduced these constructs into the wild-type strain Vd991 by *Agrobacterium*-mediated transformation, obtaining six independent transformants (Figs. 8A, B and S3A). Virulence assays showed that inoculations with OE-*lncRNA012077* transformants resulted in enhanced severity of Verticillium wilt in cotton compared with the wild-type strain Vd991 (Fig. 8C). The biomass of OE-*lncRNA012077* transformants in infected cotton tissue was significantly higher than that of the wild type strain in inoculated cotton plants (Fig. 8E). The virulence of OE-*lncRNA009491* transformants was lower as also the fungal biomass in the infected tissue (Fig. 8D and F). Moreover, OE-*lncRNA007722* transformants slightly reduced the virulence compared with Vd991 (Fig. S3B and C). However, other lncRNAs OE transformantswere unable to influence the virulence of *V. dahliae* (Fig. S3B and C). These results suggest that, depending on the lncRNA type, lncRNAs serve as both a positive and negative regulators of virulence in *V. dahliae*.

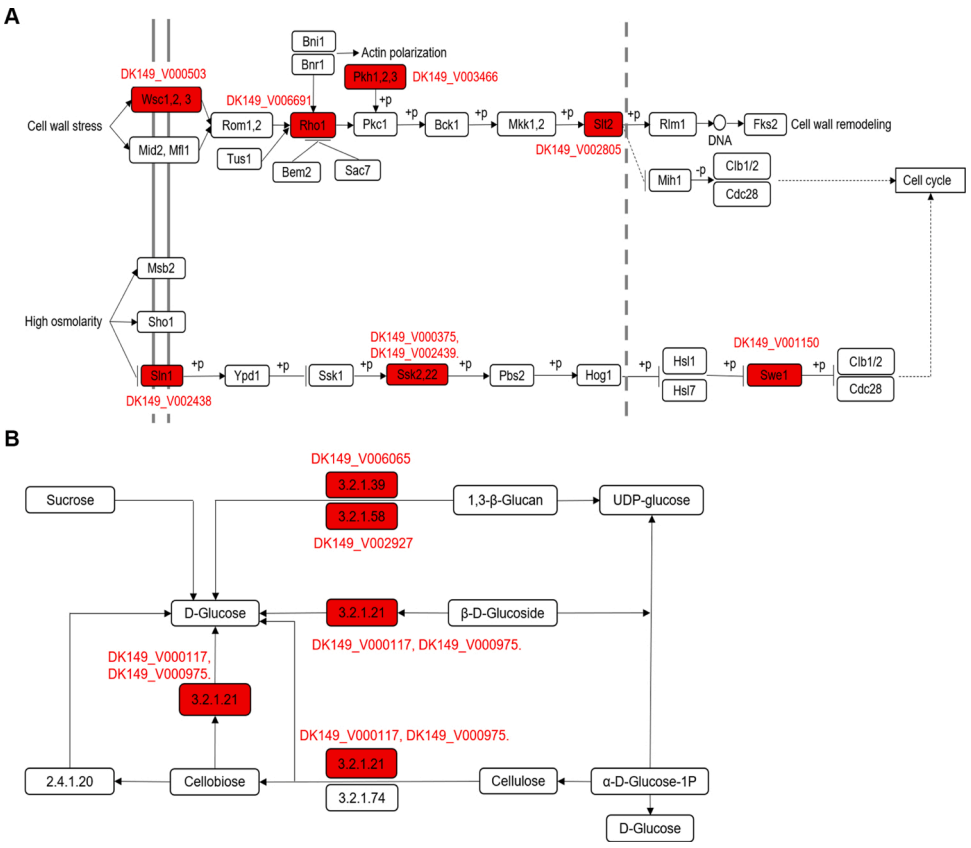

Fig. 5. Kyoto encyclopedia of genes and genomes (KEGG) pathway analysis of 308 protein-coding genes from *Verticillium dahliae* that are located within 10 kb upstream and downstream of long noncoding RNAs (lncRNAs). (**A**) Starch and sucrose metabolism of lncRNA-associated genes. (**B**) Mitogen-activated protein kinase (MAPK) signaling pathway analysis of lncRNA-associated genes.

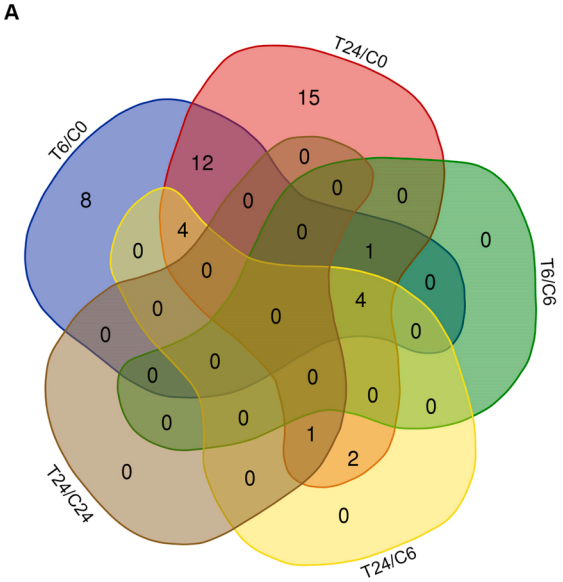

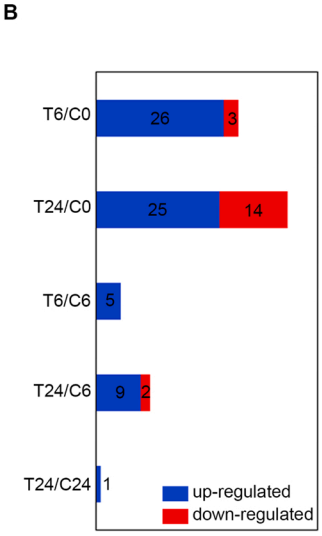

Fig. 6. Differential expression of lncRNAs from *Verticillium dahliae* following inoculation of cotton. **(A)** Venn diagram showing non-overlap and overlap of differentially expressed lncRNAs (DELs). **(B)** Number of up- and downregulated DELs in the treatment (T) versus the control (C) groups T6/C0, T24/C0, T6/C6, T24/C6, T24/C24, respectively. "C" indicates the control in which conidia of Vd991 were not inoculated onto cotton, while "T" represents conidia the treatment group in which conidia of *V. dahliae* strain Vd991 were inoculated onto cotton *Gossypium hirsutum* cultivar Junmian 1 for 0 h, 6 h, and 24 h. Thus T6/C0 refers to the 6 h treatment group in comparison to the control group at 0 h, etc.

4. Discussion

A total of 352 lncRNAs were identified in *V. dahliae*. Although the strict criteria for identification of *V. dahliae* lncRNAs were similar to those used in previous studies (Cai et al., 2018; Salih et al., 2019; Ma et al., 2019; Wang et al., 2017), comparison of multiple time points (0 h, 6 h, and 24 h) during normal development and when inoculated on cotton enabled the discovery of many novel lncRNA transcripts (Fig. 1). Though most lncRNAs were described in humans and other mammals initially (Ponting et al., 2009; Guttman and Rinn, 2012), the list of lncRNAs uncovered in this study will help guide related research in *V. dahliae* and other fungi. We also studied the distinct characteristics of lncRNAs in *V. dahliae*, such as length, exon number, length of ORF, GC%, and their potential functions in *V. dahliae*.

Table 1
List of neighbouring genes that associate with differentially expressed lncRNAs.

Gene-ID	Chromosome-ID	Star	End	Flank	Length	eggNOG_define	Secretome	SCRPs	Cysteine-rich	CAZymes	cellulose	hemicellulose	Transcription factor	PHI ID
DK149_V000020	ch01	63598	65115	+	1518	NA								
DK149_V000375	ch01	1098965	1100786	–	1822	solute carrier family 22								PHI:3381
DK149_V000376	ch01	1101718	1103098	–	1381	RNA binding								
DK149_V000603	ch01	1850517	1857008	+	6492	ATPase activity, coupled to transmembrane movement of substances								PHI:1018 PHI:2042
DK149_V001139	ch01	3556865	3557537	+	673	sequence-specific DNA binding							Lambda repressor-like, DNA-binding// Helix-turn-helix type 3	PHI:4107
DK149_V001155	ch01	3624713	3625177	–	465	Clock-controlled protein 6	Y	Y	Y					
DK149_V001156	ch01	3629254	3630637	+	1384	oxidoreductase activity								PHI:714
DK149_V002351	ch01	7612222	7613166	–	945	zinc ion binding			Y					
DK149_V002352	ch01	7613786	7616968	+	3183	damaged DNA binding								
DK149_V002382	ch01	7702149	7704006	–	1858	oxidoreductase activity, acting on NAD(P)H, oxygen as acceptor								PHI:6640
DK149_V002437	ch02	73322	76272	+	2951	Carbohydrate esterase family 9 protein								PHI:4840
DK149_V002438	ch02	77030	81446	+	4417	monocarboxylate transporter							Zn2Cys6	PHI:812
DK149_V002439	ch02	81587	84949	–	3363	Transcription factor	Y						Zn2Cys6	PHI:1755
DK149_V003221	ch02	2891691	2894300	–	2610	secondary active sulfate transmembrane transporter activity								PHI:6554
DK149_V003258	ch02	3053781	3056873	–	3093	L-alpha-amino acid transmembrane transport								
DK149_V003468	ch02	3719638	3733265	+	13,628	vacuolar proton-transporting V-type ATPase complex assembly								PHI:2352 PHI:2354
DK149_V003476	ch02	3927734	3931377	–	3644	Nuclear cap-binding protein subunit 3								
DK149_V003612	ch02	4384757	4386589	+	1833	Lipase (class 3)								
DK149_V004144	ch03	1225665	1226661	+	997	negative regulation of SMAD protein signal transduction								
DK149_V004145	ch03	1226949	1229181	–	2233	nuclear localization sequence binding								
DK149_V004150	ch03	1255916	1257276	+	1361	mannose-1-phosphate guanylyltransferase activity			Y					PHI:5344
DK149_V004273	ch03	1656948	1660118	–	3171	sinapyl alcohol dehydrogenase activity								PHI:5572
DK149_V004274	ch03	1662117	1663405	–	1289	glycoside hydrolase family 16 protein	Y			GH16;				
DK149_V004527	ch03	2712708	2714087	+	1380	L-threonylcarbamoyladenylate synthase								PHI:7155
DK149_V004729	ch03	3391453	3393113	+	1661	Nitrate transporter								PHI:1086
DK149_V005140	ch04	338984	340054	+	1071	carboxylic ester hydrolase activity			Y	CE10;				
DK149_V005182	ch04	459483	460006	+	524	GTP binding								PHI:7009
DK149_V005183	ch04	461168	466131	+	4964	actin filament capping								
DK149_V005330	ch04	995610	997320	–	1711	protein deneddylation								
DK149_V005411	ch04	1286037	1288092	+	2056	inorganic phosphate transmembrane transporter activity								PHI:3528
DK149_V005646	ch04	2065356	2066486	–	1131	FMN binding								
DK149_V005990	ch04	3283270	3285158	–	1889	pyruvate decarboxylase activity								

(*continued on next page*)

Table 1 (*continued*)

Gene-ID	Chromosome-ID	Star	End	Flank	Length	eggNOG_define	Secretome	SCRPs	Cysteine-rich	CAZymes	cellulose	hemicellulose	Transcription factor	PHI ID
DK149_V005991	ch04	3286229	3286910	–	682	flavin-linked sulfhydryl oxidase activity			Y					
DK149_V006154	ch05	77729	78793	+	1065	Galactosyl transferase GMA12 MNN10 family protein			Y	GT34;				
DK149_V006398	ch05	847201	848942	–	1742	Glutathione S-transferase, N-terminal domain								
DK149_V006399	ch05	850737	851608	–	872	carbonate dehydratase activity	Y							
DK149_V006448	ch05	1009376	1014577	–	5202	clathrin-dependent endocytosis								PHI:773 PHI:791 PHI:2141
DK149_V006471	ch05	1262869	1263844	+	976	regulation of plasma membrane sterol distribution			Y					
DK149_V006472	ch05	1264159	1264517	–	359	subunit e								
DK149_V006816	ch05	2363830	2367461	–	3632	NA								
DK149_V006817	ch05	2368053	2369470	–	1418	carboxylic ester hydrolase activity				CE10;	Y	Y		PHI:7115
DK149_V006984	ch05	2925292	2926426	+	1135	sinapyl alcohol dehydrogenase activity			Y					PHI:5034
DK149_V008108	ch06	2960126	2960467	+	342	Serine threonine-protein kinase sgk2								
DK149_V008419	ch07	302539	307142	+	4604	ATPase activity								PHI:1030
DK149_V009095	ch07	2691640	2693136	–	1497	succinate-semialdehyde dehydrogenase (NAD+) activity								PHI:3914
DK149_V009335	ch08	77151	78648	–	1498	zinc ion transmembrane transporter activity								PHI:2107
DK149_V009715	ch08	1233960	1238306	+	4347	phosphorelay sensor kinase activity								PHI:7569
DK149_V009971	ch08	2205484	2207379	–	1896	ligase activity								PHI:7486
DK149_V010032	ch08	2403812	2405673	+	1862	tripeptidyl peptidase A	Y							
DK149_V010036	ch08	2431146	2432707	+	1562	negative regulation of gluconeogenesis								
DK149_V010037	ch08	2433511	2435639	–	2129	exonucleolytic nuclear-transcribed mRNA catabolic process involved in deadenylation-dependent decay								
DK149_V010255	ch08	3154804	3156372	–	1569	oxygen carrier activity								PHI:3275
DK149_V010256	ch08	3268363	3157681	+	817	–			Y					

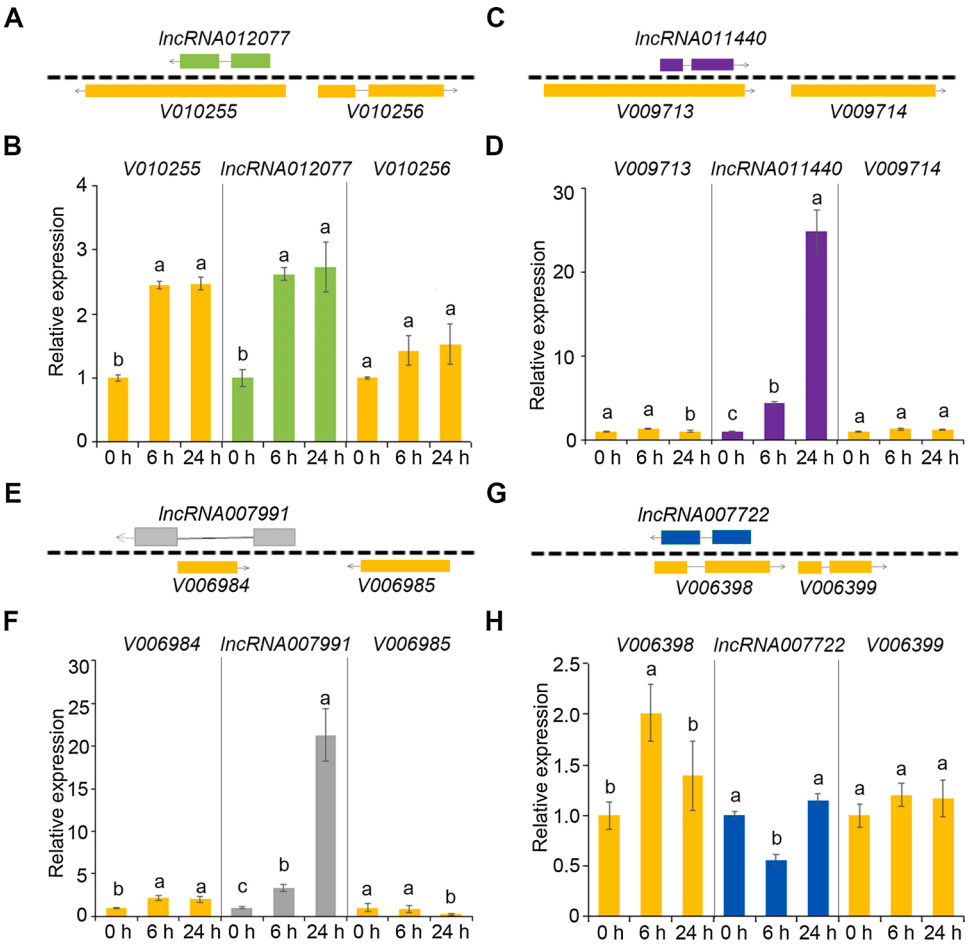

Fig. 7. Expression analysis of the long non-coding RNAs (lncRNAs) of *Verticillium dahliae* and neighboring putative *cis*-targeted genes. (**A**) Characteristics of *lncRNA012077* and its neighboring genes. (**B**) Expression of genes detected by reverse transcription-quantitative PCR (RT-qPCR). (**C**) Characteristics of *lncRNA007722* and its neighboring genes. (**D**) Expression of genes detected by RT-qPCR. Relative expression levels were normalized by *V. dahliae* elongation factor *VdEF-1α* expression level. The relative lncRNA expression level in the non-inoculated control group at timepoint 0 (C0) and the treatment group of *V. dahliae* strain Vd991 inoculated onto cv. Junmian No.1 at timepoint 0 (T0) was assigned a value of 1.0. The other time points specified include 6 h and 24 h. Error bars indicate ±SD of three biological replicates, with each measured in triplicate. Samples marked with different letters show a significant difference at $P < 0.05$.

Based on the current knowledge gleaned from the literature, the characteristics of fungal lncRNAs are similar to those described in mammals and plants (Till et al., 2018). However, in *V. dahliae*, 352 lncRNAs were of shorter length, contained lower exon number, GC content, and shorter ORFs (Fig. 2) than the lncRNAs previously discovered (Till et al., 2018). The identified lncRNAs were widely transcribed from every *V. dahliae* chromosome. However, in addition to the expression patterns, RNA secondary structure, DNA conservation, and epigenetic signatures such as H3K4me3 histone modifications have been used to identify non-coding RNAs in humans and mice (Guttman et al., 2009). While the structure and level of conservation of lncRNAs are considerably different between those from animals and plants (Di et al., 2014), the differences in lncRNAs between fungi and other species remain unknown.

Validating the functions of lncRNAs represents a major challenge in understanding RNA-mediated gene regulation. Although genome-wide transcriptome analyses have identified thousands of lncRNAs that likely serve as versatile regulators of diverse physiological and pathological functions, the functions of the vast majority of lncRNAs are undetermined. Some lncRNAs are derived from transposable elements (TEs) or contain remnants of TEs. Also, unlike miRNAs or proteins, the function of lncRNAs cannot currently be inferred from their sequence or structure. Evidence suggests that antisense lncRNAs may be involved in the regulation of the expression of either their neighboring genes in *cis* or more distant genes in *trans* states through various mechanisms (Ponting et al., 2009). Two lncRNAs were identified to target genes in *cis*, and to regulate pathogenicity and growth in fungal plant pathogens. *UvlncNAT-MFS* participates in the regulation of *U.virens* growth, conidiation, and various stress responses by forming RNA duplexes with *UvMFS* (Tang et al., 2021). *GzmetE-AS* transcribed from the opposite strand of *GzmetE* was identified to participate in *F.graminearum* asexual and sexual reproduction by regulating the expression of *GzmetE* (Wang et al., 2021). In this study, neighboring genes of lncRNAs regarded as putative *cis*-targeted genes of lncRNAs were predicted (Table S4). We performed a GO analysis to understand the functions of the potential *cis*-targeted genes from the lncRNAs identified. Potential *cis*-targeted genes mainly participated in transferase activity, oxidoreductase activity, hydrolase activity, and nitrogen compound metabolic process. LncRNA mainly functions as an indirect regulator by binding DNA, RNA, or protein. Putative target genes of lncRNAs in *V. dahliae* were mainly related to binding which may act on RNA, protein, and DNA. Several plant lncRNAs have been verified to regulate immune responses (Di et al., 2014; Seo et al., 2019). Herein, some genes were enriched in response to stimuli, stress, and chemicals. Furthermore, two genes were related to eukaryotic translation initiation factor 3 complex (eIF-3 complex) in their cell component (Fig. 4D). The eIF-3 complex is involved in the protein synthesis from a specialized repertoire of mRNAs together with other initiation factors that stimulate binding of mRNA and methionyl-tRNAi to the 40S ribosome (Gomes-Duarte et al., 2018). Together with other initiation factors and those that stimulate binding of mRNA and methionyl-tRNAi to the 40S ribosome, the eIF-3 complex specifically targets and initiates translation of a subset of mRNAs involved in cell proliferation (Gomes-Duarte et al., 2018). Potentially, *V. dahliae* lncRNAs also modulate the growth and development of the pathogen.

In this study, differentially expressed lncRNAs were discovered in a time course following inoculation (0 h, 6 h, and 24 h), suggesting that *V. dahliae* lncRNAs can function during early interactions with the host and potentially during infection (Fig. 6). Many genes related to pathogenicity were significantly differentially expressed following

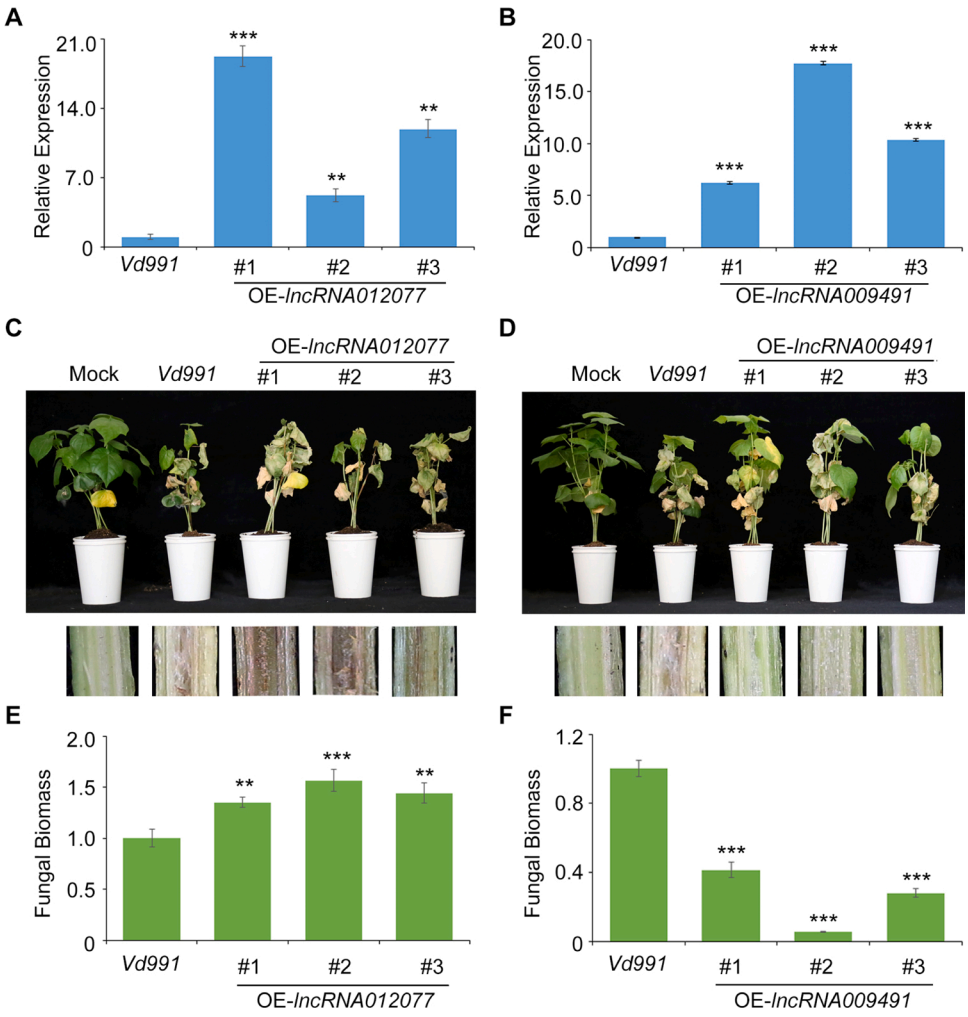

Fig. 8. Pathogenicity analysis of *Verticillium dahliae* overexpressing long noncoding RNAs (lncRNAs). (**A, B**) Reverse transcription-quantitative PCR detected the expression of *lncRNA012077* in *lncRNA012077*-over-expressing transformants (OE-*lncRNA012077*) and *lncRNA009491* in *lncRNA009491* over-expressing transformants (OE-*lncRNA009491*). (**C, D**) Phenotypes of cotton seedlings inoculated with OE-*lncRNA012177* and OE-*lncRNA009491*, respectively. Two-week-old seedlings of susceptible cotton (cv. Junmian No.1) were inoculated with sterile water (Mock), wild-type *V. dahliae* (Vd991), and three independent overexpression strains. The disease symptoms 3 weeks after inoculation are shown at the top, and the discoloration of the inoculation shoot longitudinal sections is shown at the bottom. (**E, F**) The fungal biomasses of the OE-*lncRNA012177* and OE-*lncRNA009491* on cotton were detected by quantitative PCR. Error bars indicate ±SD of three biological replicates, with each measured in triplicate. Samples marked with asterisk show a significant difference at $P < 0.01$ (**) and $P < 0.001$ (***).

inoculation with *V. dahliae*, including transcription factors, components of secretome, and other enzymes (Zhou et al., 2012; Santhanam et al., 2013; Liu et al., 2014; Zhang et al., 2018a, 2018b). The lncRNAs also function by regulating the expression of other genes. The genes neighboring the identified lncRNAs included components of the secretome, SCRP, kinase, transcription factors, and CAZy-types with CMB, AA, GH, GT, and CE activities (Table 1). Four of the lncRNAs were differentially expressed following inoculation onto cotton, and the expression patterns of their neighboring genes may indicate lncRNA-mediated regulation (Fig. 7). Overexpression of *lncRNA012077* enhanced the virulence of *V. dahliae* on cotton, while, overexpression *lncRNA009491* reduced the virulence of *V. dahliae* on cotton (Fig. 8). These results suggest that lncRNA serve as both positive or negative regulators of virulence in *V. dahliae*. Above all, *V. dahliae* lncRNA may play a role in the pathogenicity by regulating the expression of various pathogenicity-related genes during infection.

Pathogenicity of *V. dahliae* is a complex process that involves a series of morphogenetic and physiological changes. This study represents the first to report on the genome-wide identification of 352 novel lncRNAs in *V. dahliae*. Many of the identified lncRNAs were differentially expressed following inoculation with *V. dahliae*. Analysis of the lncRNAs and their putative *cis*-targeted genes suggest that lncRNAs may also play important roles in the virulence of *V. dahliae*. Previous studies have shown that small RNAs have functions in *V. dahliae* (Jin et al., 2018, 2019). *V. dahliae* infection caused upregulation in the expression of two endogenous plant miRNAs that were exported to fungal cells to silence virulence genes (Jin et al., 2018). Our results provide new insights into the functioning of lncRNA during *V. dahliae* infection and, therefore may offer a new approach to reduce the virulence of *V. dahliae* to prevent crop yield losses.

Data availability

The data presented in this article have been deposited in the National Center for Biotechnology Information (NCBI) Sequence Read Archive (http://www.ncbi.nlm.nih.gov/sra/, accession number is PRJNA735544).

All foci coordinates, activation probability maps, in addition to the supplemental information will be available on ANIMA: a data-sharing initiative for neuro-imaging meta-analyses:anima.fz-juelich.de.

Author statement

Steven J. Klosterman and Xiao-Feng Dai conceived this research. Ran Li and Jie-Yin Chen designed and directed the study. Hui-Shan Xue, Dan-Dan Zhang, Dan Wang, and Jian Song assisted with specific experiments. Ran Li and Jie-Yin Chen prepared the manuscript and edited by Krishna V. Subbarao and Steven J. Klosterman. None of the authors have conflicts of interest with this manuscript. All authors have read and agreed to the published version of the manuscript.

Acknowledgments

This work was supported by the National Natural Science Foundation

of China (32001862, 31870138), the National Key Research and Development Program of China (2018YFE0112500), the Elite Youth Program CAAS to J.Y.C., the Agricultural Science and Technology Innovation Program grant to X.F.D.

Appendix A. Supplementary data

Supplementary material related to this article can be found, in the online version, at doi:https://doi.org/10.1016/j.micres.2022.126962.

References

Anderson, D.M., Anderson, K.M., Chang, C., Makarewich, C.A., Nelson, B.R., McAnally, J. R., et al., 2015. A micropeptide encoded by a putative long noncoding RNA regulates muscle performance. Cell. 160, 595–606.

Beaulieu, Y.B., Kleinman, C.L., Landry-Voyer, A.M., Majewski, J., Bachand, F., 2012. Polyadenylation-dependent control of long noncoding RNA expression by the poly (A)-binding protein nuclear 1. PLoS Genet. 8, e1003078.

Cabili, M.N., Trapnell, C., Goff, L., Koziol, M., Tazon-Vega, B., Regev, A., 2011. Integrative annotation of human large intergenic noncoding RNAs reveals global properties and specific subclasses. Genes Dev. 25, 1915–1927.

Cai, W., Li, C., Liu, S., Zhou, C., Yin, H., Song, J., et al., 2018. Genome wide identification of novel long non-coding RNAs and their potential associations with milk proteins in Chinese holstein cows. Front. Genet. 9, 281.

Chen, J.Y., Liu, C., Gui, Y.J., Si, K.W., Zhang, D.D., Wang, J., et al., 2018. Comparative genomics reveals cotton-specific virulence factors in flexible genomic regions in *Verticillium dahliae* and evidence of horizontal gene transfer from Fusarium. New Phytol. 217, 756–770.

Csorba, T., Questa, J.I., Sun, Q., Dean, C., 2014. Antisense *COOLAIR* mediates the coordinated switching of chromatin states at FLC during vernalization. Proc. Natl. Acad. Sci. U.S.A. 111, 16160–16165.

de Jonge, R., Bolton, M.D., Kombrink, A., van den Berg, G.C.M., Yadeta, K.A., Thomma, B.P.H.J., 2013. Extensive chromosomal reshuffling drives evolution of virulence in an asexual pathogen. Genome Res. 23, 1271–1282.

Di, C., Yuan, J., Wu, Y., Li, J., Lin, H., Hu, L., et al., 2014. Characterization of stress-responsive lncRNAs in *Arabidopsis thaliana* by integrating expression, epigenetic and structural features. Plant J. 80, 848–861.

Fradin, E.F., Thomma, B.P.H.J., 2006. Physiology and molecular aspects of Verticillium wilt diseases caused by *V. dahliae* and *V. alboatrum*. Mol. Plant Pathol. 7, 71–86.

Gomes-Duarte, A., Lacerda, R., Menezes, J., Romão, L., 2018. eIF3: a factor for human health and disease. RNA Biol. 15, 26–34.

Gui, Y.J., Chen, J.Y., Zhang, D.D., Li, N.Y., Li, T.G., Zhang, W.Q., et al., 2017. *Verticillium dahliae* manipulates plant immunity by glycoside hydrolase 12 proteins in conjunction with carbohydrate-binding module 1. Environ. Microbiol. 19, 1914–1932.

Guo, H., Wang, X., Gundlach, H., Mayer, K.F.X., Peterson, D.G., Scheffler, B.E., et al., 2014. Extensive and biased intergenomic nonreciprocal DNA exchanges shaped a nascent polyploid genome, *Gossypium* (Cotton). Genetics 197, 1153–1163.

Guttman, M., Rinn, J.L., 2012. Modular regulatory principles of large non-coding RNAs. Nature 482, 339–346.

Guttman, M., Amit, I., Garber, M., French, C., Lin, M.F., Feldser, D., et al., 2009. Chromatin signature reveals over a thousand highly conserved large non-coding RNAs in mammals. Nature 458, 223–227.

Guttman, M., Russell, P., Ingolia, N.T., Weissman, J.S., Lander, E.S., 2013. Ribosome profiling provides evidence that large noncoding RNAs do not encode proteins. Cell 154, 240–251.

Jin, Y., Zhao, P., Fang, Y., Gao, F., Guo, H., Zhao, J., 2018. Genome-wide profiling of sRNAs in the *Verticillium dahliae*-infected *Arabidopsis* roots. Mycology 9, 155–165.

Jin, Y., Zhao, J., Zhao, P., Zhang, T., Wang, S., Guo, H., 2019. A fungal milRNA mediates epigenetic repression of a virulence gene in *Verticillium dahliae*. Philos. Trans. Biol. Sci. 374, 20180309.

Johnsson, P., Lipovich, L., Grandér, D., Morris, K.V., 2014. Evolutionary conservation of long non-coding RNAs; sequence, structure, function. BBA-Gen Subjects 1840, 1063–1071.

Kanehisa, M., Sato, Y., Furumichi, M., Morishima, K., Tanabe, M., 2019. New approach for understanding genome variations in KEGG. Nucleic Acids Res. 47, D590–D595.

Kim, D., Pertea, G., Trapnell, C., Pimentel, H., Kelley, R., Salzberg, S.L., 2013. TopHat2: accurate alignment of transcriptomes in the presence of insertions, deletions and gene fusions. Genome Biol. 14, R36.

Klimes, A., Dobinson, K.F., Thomma, B.P.H.J., Klosterman, S.J., 2015. Annu. Rev. Phytopathol. 53, 181–198.

Klosterman, S.J., Subbarao, K.V., Kang, S., Veronese, P., Gold, S.E., Thomma, B.P.H.J., et al., 2011. Comparative genomics yields insights into niche adaptation of plant vascular wilt pathogens. PLoS Pathog. 7, e1002137.

Langmead, B., Salzberg, S.L., 2012. Fast gapped-read alignment with bowtie 2. Nat. Methods 9, 357–359.

Li, N., Ma, X., Short, D.P.G., Li, T., Zhou, L., Gui, Y., et al., 2018a. The island cotton NBS-LRR gene GbaNA1 confers resistance to the non-race 1 *Verticillium dahliae* isolate Vd991. Mol. Plant Pathol. 19, 1466–1479.

Li, R., Fu, D., Zhu, B., Luo, Y., Zhu, H., 2018b. CRISPR/Cas9-mediated mutagenesis of *lncRNA1459* alters tomato fruit ripening. Plant J. 94, 513–524.

Li, R., Zhu, H.L., Luo, Y.B., 2016. Understanding the Functions of Long Non-Coding RNAs through Their Higher-Order Structures. Int. J. Mol. Sci. 17, 702.

Liu, T., Song, T., Zhang, X., Yuan, H., Su, L., Li, W., et al., 2014. Unconventionally secreted effectors of two filamentous pathogens target plant salicylate biosynthesis. Nat. Commun. 5, 4686.

Luke, B., Panza, A., Redon, S., Iglesias, N., Li, Z., Lingner, J., 2008. The Rat1p 5' to 3' exonuclease degrades telomeric repeat-containing RNA and promotes telomere elongation in saccharomyces cerevisiae. Mol. Cell 32, 465–477.

Ma, J., Bai, X., Luo, W., Feng, Y., Shao, X., Bai, Q., et al., 2019. Genome-wide identification of long noncoding RNAs and their responses to salt stress in two closely related poplars. Front. Genet. 10, 777.

Mercer, T.R., Mattick, J.S., 2013. Structure and function of long noncoding RNAs in epigenetic regulation. Nat. Struct. Mol. Biol. 20, 300–307.

Nelson, B.R., Makarewich, C.A., Anderson, D.M., Winders, B.R., Troupes, C.D., Wu, F., et al., 2016. A peptide encoded by a transcript annotated as long noncoding RNA enhances SERCA activity in muscle. Science 351, 271–275.

Ponting, C.P., Oliver, P.L., Reik, W., 2009. Evolution and functions of long noncoding RNAs. Cell 136, 629–641.

Qin, T., Zhao, H., Cui, P., Albesher, N., Xiong, L., 2017. A nucleus-localized long non-coding RNA enhances drought and salt stress tolerance. Plant Physiol. 175, 1321–1336.

Salih, H., Gong, W., He, S., Xia, W., Odongo, M.R., Du, X., 2019. Long non-coding RNAs and their potential functions in Ligon-lintless-1 mutant cotton during fiber development. BMC Genomics 20, 661.

Santhanam, P., van Esse, H.P., Albert, I., Faino, L., Nürnberger, T., Thomma, B.P.H.J., 2013. Evidence for functional diversification within a fungal NEP1-Like protein family. Mol. Plant Microbe In. 26, 278–286.

Seo, J.S., Diloknawarit, P., Park, B.S., Chua, N.H., 2019. ELF18-INDUCED LONG NONCODING RNA 1 evicts fibrillarin from mediator subunit to enhance PATHOGENESIS-RELATED GENE 1 (PR1) expression. New Phytol. 221, 2067–2079.

Sun, Y., Liu, W., Liu, T., Feng, X., Yang, N., Zhou, H., 2015. Signaling pathway of MAPK/ERK in cell proliferation, differentiation, migration, senescence and apoptosis. J. Recept. Signal Transduct. Res. 35, 600–604.

Tang, J., Chen, X., Yan, Y., Huang, J., Luo, C., Tom, H., et al., 2021. Comprehensive transcriptome profiling reveals abundant long non-coding RNAs associated with development of the rice false smut fungus, *Ustilaginoidea virens*. Environ. Microbiol. https://doi.org/10.1111/1462-2920.15432.

Till, P., Mach, R.L., Mach-Aigner, A.R., 2018. A current view on long noncoding RNAs in yeast and filamentous fungi. Appl Microbiol Biot. 102, 7319–7331.

Till, P., Derntl, C., Kiesenhofer, D.P., Mach, R.L., Yaver, D., Mach-Aigner, A.R., 2020. Regulation of gene expression by the action of a fungal lncRNA on a transactivator. RNA Biol. 17, 47–61.

Trapnell, C., Williams, B.A., Pertea, G., Mortazavi, A., Kwan, G., van Baren, M.J., et al., 2010. Transcript assembly and quantification by RNA-Seq reveals unannotated transcripts and isoform switching during cell differentiation. Nat. Biotechnol. 28, 511–515.

Ulitsky, I., Bartel, D.P., 2013. lincRNAs: genomics, evolution, and mechanisms. Cell 154, 26–46.

van Werven, F.J., Neuert, G., Hendrick, N., Lardenois, A., Buratowski, S., van Oudenaarden, A., et al., 2012. Transcription of two long noncoding RNAs mediates mating-type control of gametogenesis in budding yeast. Cell 150, 1170–1181.

Villegas, V., Zaphiropoulos, P., 2015. Neighboring gene regulation by antisense long non-coding RNAs. Int. J. Mol. Sci. 16, 3251–3266.

Wang, C., Liu, S., Zhang, X., Ma, Y., Hu, C., Zhang, J., 2017. Genome-wide screening and characterization of long non-coding RNAs involved in flowering development of trifoliate orange (Poncirus trifoliata L. Raf.). Sci. Rep. 7, 43226.

Wang, Y., Luo, X., Sun, F., Hu, J., Zha, X., Su, W., et al., 2018. Overexpressing lncRNA LAIR increases grain yield and regulates neighbouring gene cluster expression in rice. Nat. Commun. 9, 3516.

Wang, J., Zeng, W., Xie, J., Fu, Y., Jiang, D., Lin, Y., et al., 2021. A novel antisense long noncoding RNA participates in asexual and sexual reproduction by regulating the expression of *GzmetE* in *Fusarium graminearum*. Environ. Microbiol. https://doi.org/10.1111/1462-2920.15399.

Wu, H.W., Deng, S., Xu, H., Mao, H.Z., Liu, J., Niu, Q.W., et al., 2018. A noncoding RNA transcribed from the AGAMOUS (AG) second intron binds to CURLY LEAF and represses AG expression in leaves. New Phytol. 219, 1480–1491.

Zappulla, D.C., Cech, T.R., 2004. Yeast telomerase RNA: a flexible scaffold for protein subunits. Proc. Natl. Acad. Sci. U.S.A. 101, 10024–10029.

Zhang, L., Wang, M., Li, N., Wang, H., Qiu, P., Pei, L., et al., 2018a. Long noncoding RNAs involve in resistance to *Verticillium dahliae*, a fungal disease in cotton. Plant Biotechnol. J. 16, 1172–1185.

Zhang, W., Gui, Y., Short, D.P.G., Li, T., Zhang, D., Zhou, L., et al., 2018b. *Verticillium dahliae* transcription factor *VdFTF1* regulates the expression of multiple secreted virulence factors and is required for full virulence in cotton. Mol. Plant Pathol. 19, 841–857.

Zhang, D.D., Wang, J., Wang, D., Kong, Z.Q., Zhou, L., Zhang, G.Y., et al., 2019. Population genomics demystifies the defoliation phenotype in the plant pathogen *Verticillium dahliae*. New Phytol. 222, 1012–1029.

Zhou, B., Jia, P., Gao, F., Guo, H., 2012. Molecular characterization and functional analysis of a necrosis- and ethylene-inducing, protein-encoding gene family from *Verticillium dahliae*. Mol. Plant-microbe Interact. 25, 964.

Zhu, Q., Stephen, S., Taylor, J., Helliwell, C.A., Wang, M., 2014. Long noncoding RNAs responsive to Fusarium oxysporum infection in *Arabidopsis thaliana*. New Phytol. 201, 574–584.